Thermodynamic limit of the six-vertex model with domain wall boundary conditions

2000 J. Phys. A: Math. Gen. 33 7053

(http://iopscience.iop.org/0305-4470/33/40/304)

J. Phys. A: Math. Gen. **33** (2000) 7053–7066. Printed in the UK PII: S0305-4470(00)14111-3

Thermodynamic limit of the six-vertex model with domain wall boundary conditions

V Korepin and P Zinn-Justin

C N Yang Institute for Theoretical Physics, State University of New York at Stony Brook, Stony Brook, NY 11794-3840, USA

Received 18 May 2000

Abstract. We address the question of the dependence of the bulk free energy on boundary conditions for the six-vertex model. Here we compare the bulk free energy for periodic and domain wall boundary conditions. Using a determinant representation for the partition function with domain wall boundary conditions, we derive Toda differential equations and solve them asymptotically in order to extract the bulk free energy. We find that it is different and bears no simple relation to the free energy for periodic boundary conditions. The six-vertex model with domain wall boundary conditions is closely related to algebraic combinatorics (alternating sign matrices). This implies new results for the weighted counting for large-size alternating sign matrices. Finally, we comment on the interpretation of our results, in particular in connection with domino tilings (dimers on a square lattice).

1. Introduction

The six-vertex model is an important model of classical statistical mechanics in two dimensions. The prototypical model is the ice model, which was solved by Lieb [1] in 1967 by means of the Bethe ansatz, followed by several generalizations [2–4]. The solution of the most general six-vertex model was given by Sutherland [5] in 1967. The bulk free energy was calculated in these papers for periodic boundary conditions (PBC). A detailed classification of the phases of the model can be found, for example, in the book [6] (see also the more recent work [7] on antiperiodic boundary conditions).

Earlier, in 1961 Kasteleyn, while studying dimer arrangements on a quadratic lattice, expressed doubts concerning the independence of the bulk free energy on boundary conditions [8]. For more on dimer arrangements, see [8–10]. Interest in this subject was renewed with recent work on domino tilings (which are equivalent to dimers on a square lattice) of an Aztec diamond [11, 12], demonstrating a strong effect of the boundary on a typical domino configuration (see also [13]). Dimers (or domino tilings) can be considered as a particular case of the six-vertex model, and therefore a natural question is to investigate the effect of boundary conditions on the thermodynamic limit of the six-vertex model.

Independently of this, new boundary conditions of the six-vertex model, the so-called domain wall boundary conditions (DWBC), were first introduced in 1982 [14] (we shall define them in detail below). An important recursion relation for the partition function was discovered in this paper. Later these recursion relations helped to find a determinant representation for the partition function of the six-vertex model with DWBC [15, 16]. The determinant representation simplifies somewhat in the homogeneous case. In this case the partition function satisfies the

0305-4470/00/407053+14$30.00

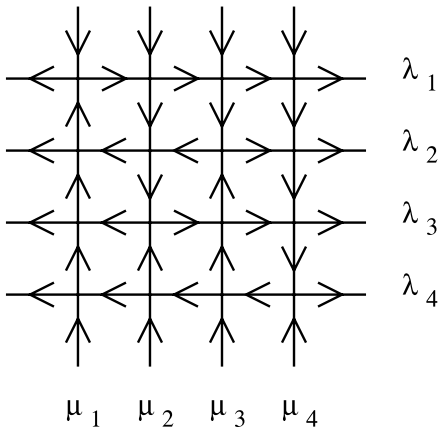

Figure 1. A configuration of the inhomogeneous six-vertex model with domain wall boundary conditions.

Toda differential equation [17]. In this paper we use this differential equation in order to calculate the bulk free energy for domain wall boundary conditions.

Let us mention that there is a one-to-one correspondence between arrow configurations in the six-vertex model with DWBC and alternating sign matrices (ASM) [18]. This mapping was used in order to count the number of ASMs. More on ASM can be found in [19, 20].

The plan of the paper is as follows. In section 2 we define the six-vertex model with domain wall boundary conditions, and derive the determinant representation for the partition function. In section 3 we derive the Toda differential equation for the partition function. In section 4 we consider the thermodynamic limit; we derive the explicit expression of the bulk free energy in the ferroelectric and disordered phases, and compare it with PBC. Finally, in section 5 we comment on the connection of our results with other subjects (ASM, domino tilings, height model) and conclude this discussion in section 6.

2. Determinant representation of the partition function of the six-vertex model

In this section we shall define the *inhomogeneous* six-vertex model with domain wall boundary conditions, and rewrite its partition function as a determinant. We will then particularize our formula to the homogeneous case.

First, we define the configurations of the model. They are given by assigning arrows to each edge of an $N \times N$ square lattice (see figure 1). The 'domain wall' boundary conditions correspond to fixing the horizontal external arrows to be outgoing and the vertical external arrows to be incoming. The partition function is then obtained by summing over all possible configurations:

$$Z = \sum_{\substack{\text{arrow} \\ \text{configurations}}} \prod_{i,k=1}^{N} w_{ik} \tag{2.1}$$

where the statistical weights w_{ik} are assigned to each *vertex* of the lattice. Since we are considering an inhomogeneous model, we need two sets of spectral parameters $\{\lambda_i\}$ and $\{\mu_k\}$ which are associated with the horizontal and vertical lines. The weight w_{ik} depends on the

arrow configuration around the vertex (i, k) and is given by

$$w_{ik} = \begin{cases} a(\lambda_i, \mu_k) \\ b(\lambda_i, \mu_k) \\ c(\lambda_i, \mu_k) \end{cases} \qquad (2.2)$$

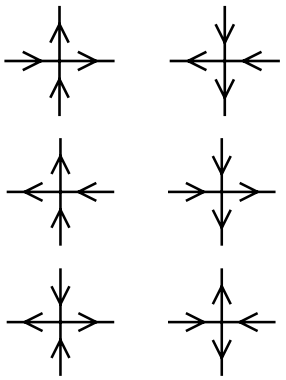

(all other weights are zero) where the functions a, b, c are chosen as follows:

$$\begin{aligned} a(\lambda, \mu) &= \sinh(\lambda - \mu - \gamma) \\ b(\lambda, \mu) &= \sinh(\lambda - \mu + \gamma) \\ c(\lambda, \mu) &= \sinh(2\gamma). \end{aligned} \qquad (2.3)$$

Here γ is an anisotropy parameter which does not depend on the lattice site. The partition function is therefore a function of the $2N$ spectral parameters and we shall denote it by $Z_N(\{\lambda_i\}, \{\mu_k\})$.

The model thus defined satisfies the following essential property (Yang–Baxter equation) shown in figure 2. The vertex with diagonal edges is assigned weights (the so-called R matrix) which are the same as the usual weights, up to a shift of the difference of the spectral parameter. Here we shall not need the explicit expression of the R matrix.

We shall now list the following four properties which entirely determine $Z_N(\{\lambda_i\}, \{\mu_k\})$ and sketch their proof (for a detailed algebraic proof the reader is referred to [16]).

(a) $Z_1 = \sinh(2\gamma)$. This is by definition.

(b) $Z_N(\{\lambda_i\}, \{\mu_k\})$ is a symmetric function of $\{\lambda_i\}$ and $\{\mu_k\}$.

It is sufficient to prove that exchange of μ_i and μ_{i+1} (for any i) leaves the partition function

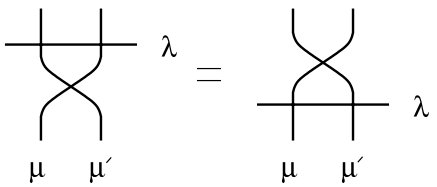

Figure 2. Yang–Baxter equation. Summation over arrows of the *internal* edges is implied, whereas external arrows are fixed.

unchanged. This can be obtained by repeated use of the Yang–Baxter property:

$$R_{\downarrow\downarrow}(\mu_i - \mu_{i+1}) Z_N(\{\dots \mu_i, \mu_{i+1} \dots\}) =$$

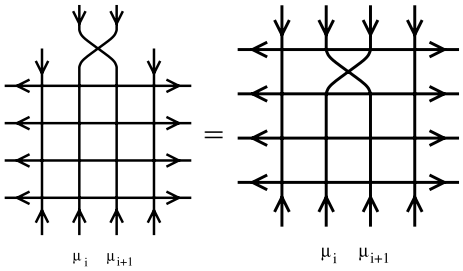

$$= \cdots =$$

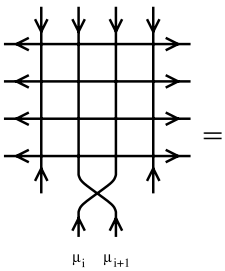

$$= R_{\uparrow\uparrow}(\mu_i - \mu_{i+1}) Z_N(\{\dots \mu_{i+1}, \mu_i \dots\}) \qquad (2.4)$$

where $R_{\uparrow\uparrow} = R_{\downarrow\downarrow}$ is the appropriate entry of the R matrix; and similarly for the $\{\lambda_i\}$.

(c) $Z_N(\{\lambda_i\}, \{\mu_k\}) = \mathrm{e}^{-(N-1)\lambda_i} P_{N-1}(\mathrm{e}^{2\lambda_i})$ where P_{N-1} is a polynomial of degree $N-1$, and similarly for the μ_k.

Let us choose one configuration. Then the only weights which depend on λ_i are the N weights on row i. Since the outgoing arrows are in opposite directions, at least one of the weights must be c. Therefore, there are at most $N-1$ weights a and b, and the product of all weights is of the form $\mathrm{e}^{-(N-1)\lambda_i} P_{N-1}(\mathrm{e}^{2\lambda_i})$. This property of course remains valid when we sum over all configurations.

(d) $Z_N(\{\lambda_i\}, \{\mu_k\})$ obeys the following recursion relation:

$$Z_N(\{\lambda_i\}, \{\mu_k\})_{|\lambda_j - \mu_l = \gamma} = \sinh(2\gamma) \prod_{\substack{1 \leqslant k \leqslant N \\ k \neq l}} \sinh(\lambda_j - \mu_k + \gamma)$$
$$\times \prod_{\substack{1 \leqslant i \leqslant N \\ i \neq j}} \sinh(\lambda_i - \mu_l + \gamma)\, Z_{N-1}(\{\lambda_i\}_{i \neq j}, \{\mu_k\}_{k \neq l}). \qquad (2.5)$$

Because of property (b), we can assume that $j = l = 1$. Since $\lambda_k - \mu_l = \gamma$ implies $a(\lambda_j - \mu_l) = 0$, by inspection all configurations with non-zero weights are of the form shown in figure 3. This immediately proves equation (2.5).

It is easy to see that the four properties (a)–(d) entirely characterize $Z_N(\{\lambda_i\}, \{\mu_k\})$. This is enough to prove that $Z_N(\{\lambda_i\}, \{\mu_k\})$ has the following determinant representation [16]:

$$Z_N(\{\lambda_i\}, \{\mu_k\}) = \frac{\prod_{1 \leqslant i,k \leqslant N} \sinh(\lambda_i - \mu_k + \gamma) \sinh(\lambda_i - \mu_k - \gamma)}{\prod_{1 \leqslant i < j \leqslant N} \sinh(\lambda_i - \lambda_j) \prod_{1 \leqslant k < l \leqslant N} \sinh(\mu_k - \mu_l)}$$
$$\times \det_{1 \leqslant i,k \leqslant N} \left[\frac{\sinh(2\gamma)}{\sinh(\lambda_i - \mu_k + \gamma) \sinh(\lambda_i - \mu_k - \gamma)} \right]. \qquad (2.6)$$

Indeed, one can check that this expression satisfies the four properties listed above.

The expression (2.6) might seem singular when two spectral parameters λ_i and λ_j coincide (and similarly for the μ_k); but, in fact, the pole created by the factor $\sinh(\lambda_i - \lambda_j)$ is compensated

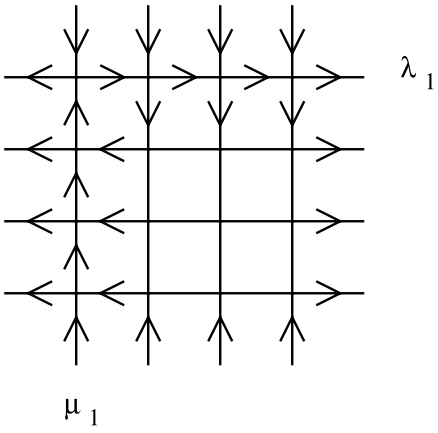

Figure 3. Graphical proof of the recursion relation.

by the zero of the determinant due to the fact that two rows are identical. Therefore, particular care must be taken when considering the homogeneous limit where all the λ_i are equal (and all the μ_k). This limit was studied in detail in [16], and we shall simply summarize the result of the calculation. Let us call t the common value of $\lambda_i - \mu_k$ for all i and k. When the λ_i are close to one another one must Taylor expand the function

$$\phi(t) \equiv \frac{\sinh(2\gamma)}{\sinh(t+\gamma)\sinh(t-\gamma)} \tag{2.7}$$

which appears in the determinant. This leads to the following expression:

$$Z_N(t) = \frac{(\sinh(t+\gamma)\sinh(t-\gamma))^{N^2}}{\left(\prod_{n=0}^{N-1} n!\right)^2} \det_{1\leqslant i,k\leqslant N}\left[\frac{\mathrm{d}^{i+k-2}}{\mathrm{d}t^{i+k-2}}\phi(t)\right]. \tag{2.8}$$

3. Determinant representation and Toda chain hierarchy

We shall now investigate the properties of the determinant which appears in equation (2.8), and for which we introduce the notation

$$\tau_N(t) = \det_{1\leqslant i,k\leqslant N}\left[m_{i+k-2}\right] \tag{3.1}$$

with

$$m_n = \frac{\mathrm{d}^n}{\mathrm{d}t^n}\phi(t). \tag{3.2}$$

Let us write down the bilinear Hirota equation satisfied by the τ_N. For completeness, we recall that they are a consequence of Jacobi's determinant identity:

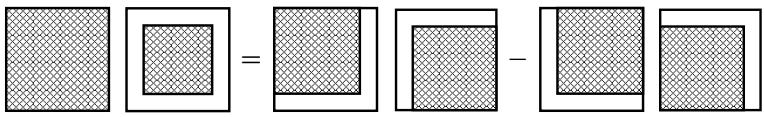

(3.3)

The large squares represent a given matrix, and the shaded regions are the sub-matrices whose determinants one must consider. Applying it to τ_{N+1} (up to a reshuffling of the rows and columns), we find [17]

$$\tau_N\tau_N'' - {\tau_N'}^2 = \tau_{N+1}\tau_{N-1} \qquad \forall N \geqslant 1 \tag{3.4}$$

where primes denote differentiation with respect to t. This is supplemented by the initial data: $\tau_0 = 1$ and $\tau_1 = \phi$. Equivalently, we have

$$(\log \tau_N)'' = \frac{\tau_{N+1}\tau_{N-1}}{\tau_N^2} \qquad \forall N \geqslant 1 \tag{3.5}$$

which is the form of the equation that we shall use.

Note that if we introduce the combinations $e^{\varphi_N} = \tau_N/\tau_{N-1}$, $N \geqslant 1$, equation (3.5) implies for the φ_N:

$$\varphi_N'' = e^{\varphi_{N+1}-\varphi_N} - e^{\varphi_N-\varphi_{N-1}} \qquad \forall N \geqslant 2 \tag{3.6}$$

and $\varphi_1'' = e^{\varphi_2-\varphi_1}$. These are the usual Toda (semi-infinite) chain equations [21–23]. Another possible form is

$$\psi_N'' = -\sum_M C_{MN}\, e^{\psi_M} \qquad N \geqslant 1 \tag{3.7}$$

with $\psi_N = \varphi_{N+1} - \varphi_N$ and C_{MN} (M, $N \geqslant 1$) the Cartan matrix of the semi-infinite diagram A_∞.

This suggests a connection with the Toda chain hierarchy [24–29]. Indeed, let us mention that given a Hänkel matrix (m_{i+k-2}), i.e. whose entries only depend on $i + k$, the m_n can be made to depend on a set of parameters $\{t_q\}_{q\geqslant 1}$ in such a way that the determinants τ_N become τ-functions of the whole Toda (semi-infinite) chain hierarchy [25]. Namely, one must choose

$$m_n(\{t_q\}) = \int d\rho(x)\, x^n\, e^{\sum_{q\geqslant 1} t_q x^q} \tag{3.8}$$

where $d\rho(x)$ is an arbitrary measure† (in the matrix model context [25], the t_q are the coefficients of the polynomial potential). Here, we are in the simplest situation where only one parameter $t_1 \equiv t$ is allowed to evolve. We immediately check that equation (3.8) implies that $m_n(t) = \frac{d^n}{dt^n} m_0(t)$, which is consistent with equation (3.2).

4. The thermodynamic limit

We shall now consider the thermodynamic (i.e. large-N) limit of the expression (2.8) in the various regimes of the six-vertex model. For that we shall use the Hirota equation in its form (3.5).

When $N \to \infty$ it is expected that the partition function behaves in the following way:

$$\log Z_N(t) = -N^2 F(t) + O(N) \tag{4.1}$$

where $F(t)$ is the *bulk free energy* (we shall always set the temperature $k_B T = 1$). Our main goal is to compute $F(t)$ explicitly.

Comparing the expected asymptotic (4.1) with the exact formula (2.8), we find that the determinant τ_N must be of the form

$$\tau_N = \left(\prod_{n=0}^{N-1} n!\right)^2 e^{N^2 f(t)+O(N)} \tag{4.2}$$

where

$$f(t) = -F(t) - \log(\sinh(t+\gamma)\sinh(t-\gamma)). \tag{4.3}$$

† This must be considered as a formal expression; e.g. the measure may not necessarily be smooth or positive.

We now want to substitute the expansion (4.2) into equation (3.5). For that we need to assume that the sub-dominant corrections to the bulk free energy vary slowly as a function of N; we shall discuss the validity of this assumption below. We then find that the expansion is consistent since both the left- and right-hand sides of (3.5) turn out to be of order N^2. The resulting equation for f is

$$f'' = \mathrm{e}^{2f}. \tag{4.4}$$

This is an ordinary second-order differential equation, which can be readily solved. The general solution depends on two parameters α and t_0:

$$\mathrm{e}^{f(t)} = \frac{\alpha}{\sinh(\alpha(t - t_0))}. \tag{4.5}$$

If the weights are chosen to be real, then the free energy should be real and this implies that α must be real or purely imaginary.

So far everything we have done was independent of the particular form of the function $\phi(t)$ and therefore independent of γ. In order to fix the two constants in (4.5), we must now discuss separately the different regimes of the six-vertex model. Let us recall that the latter are usually distinguished by the value of the parameter (cf equation (8.3.21) of [6])

$$\Delta = \frac{a^2 + b^2 - c^2}{2ab}. \tag{4.6}$$

The weights a, b, c were defined in equation (2.3) (with $\lambda - \mu \equiv t$). In this parametrization,

$$\Delta = \cosh(2\gamma). \tag{4.7}$$

4.1. Ferro-electric phase: $\Delta > 1$

This corresponds to the parameters γ and t real; we recall that the weights are given by

$$a = \sinh(t - \gamma) \qquad b = \sinh(t + \gamma) \qquad c = \sinh(2\gamma) \tag{4.8}$$

with $|\gamma| < t$. This is the so-called ferroelectric phase. In the case of periodic boundary conditions, it is known that the system is frozen in its ground state configuration, in which all arrows are aligned: if $a > b$ all arrows point up and to the right or down and to the left, whereas if $b > a$ they point up and to the left or down and to the right. The domain wall boundary conditions do not allow all arrows to be aligned: the ground state will instead take the form of figure 4. However, at leading order in the large-N limit, this does not affect the free energy, and we expect to find the same result as for periodic boundary conditions.

Indeed, it is easy to see that the relevant solution of equation (4.4) is

$$\mathrm{e}^{f(t)} = \frac{1}{\sinh(t - |\gamma|)} \tag{4.9}$$

and therefore the bulk free energy takes the form

$$\mathrm{e}^{-F(t)} = \sinh(t + |\gamma|) = \max(a, b) \tag{4.10}$$

in agreement with the case of periodic boundary conditions.

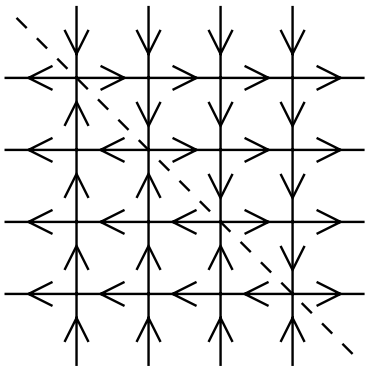

Figure 4. Ground state configuration of the ferroelectric phase (for $b > a$; the case $a > b$ is obtained by taking the mirror image).

4.2. Disordered phase: $-1 < \Delta < 1$

In this regime, it is customary to make the following redefinitions:

$$\gamma' = \mathrm{i}(\gamma + \mathrm{i}\pi/2) \tag{4.11}$$

$$t' = \mathrm{i}(t + \mathrm{i}\pi/2) \tag{4.12}$$

and divide all the weights by i, so that they take the form

$$a = \sin(\gamma - t) \qquad b = \sin(\gamma + t) \qquad c = \sin(2\gamma) \tag{4.13}$$

and $\Delta = -\cos(2\gamma)$. Using symmetry considerations, one can always assume $0 < \gamma < \pi/2$. We only consider the region $|t| < \gamma$ (where the weights are positive).

Taking into account these redefinitions, the partition function becomes

$$Z_N(t) = \frac{(\sin(t+\gamma)\sin(t-\gamma))^{N^2}}{\left(\prod_{n=0}^{N-1} n!\right)^2} \det_{1\leqslant i,k\leqslant N}\left[\frac{\mathrm{d}^{i+k-2}}{\mathrm{d}t^{i+k-2}}\phi(t)\right] \tag{4.14}$$

with a redefined $\phi(t) = \sin(2\gamma)/(\sin(t-\gamma)\sin(t+\gamma))$; the determinant τ_N still satisfies equation (3.4) and $f(t)$ defined by (4.3) is still a solution of equation (4.4)†.

Let us mention that the partition function has been computed exactly [30] at three particular values of the parameters: $t = 0$, $\gamma = \pi/6$, $\pi/4$ and $\pi/3$. In all three cases the expansion (4.1) and the assumption of smoothness of the sub-dominant corrections (which is necessary to derive the ordinary differential equation (4.4)) can be checked exactly. We have also checked it numerically for a variety of values of t and γ.

We must now select the appropriate solution (of the form (4.5)) of the equation (4.4). Let us first assume that $|t| < \gamma$ (this is the only physical region, i.e. where all the weights are positive). It is easy to check that $f(t)$ must be an even function of t. The only even solution of equation (4.4) is

$$\mathrm{e}^{f(t)} = \frac{\alpha}{\cos(\alpha t)} \tag{4.15}$$

where α remains to be determined. Note that this implies for $F(t)$

$$\mathrm{e}^{-F(t)} = \sin(\gamma - t)\sin(\gamma + t)\frac{\alpha}{\cos(\alpha t)}. \tag{4.16}$$

† Note that the sign is unchanged in equation (4.4); this is the combined effect of the 'Wick rotation' of t ($t \to \mathrm{i}t$) and of dividing all the weights by i ($\mathrm{e}^f \to -\mathrm{i}\,\mathrm{e}^f$).

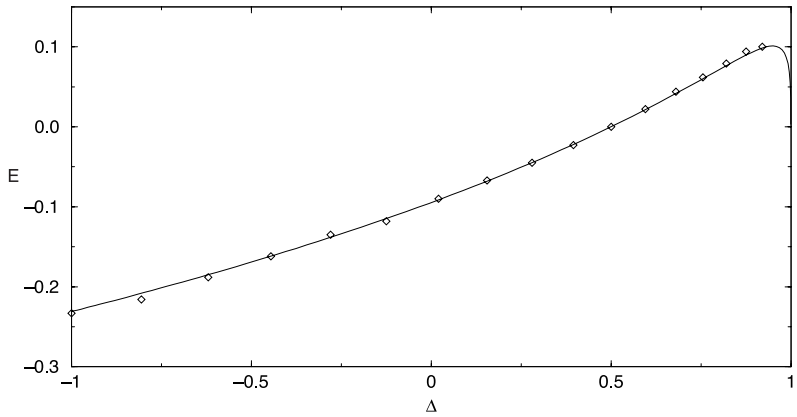

Figure 5. Energy E as a function of the anisotropy Δ. The curve is given by equation (4.21), whereas the diamonds are the results of Monte Carlo simulations on lattices of size $N = 64$.

We must then use the boundary condition given by $t = \pm\gamma$. At these values one can compute $Z_N(t)$ directly. Indeed, the only non-zero configurations are of the form of figure 4, and we find

$$Z_N(t = \pm\gamma) = \sin(2\gamma)^{N^2} \tag{4.17}$$

and therefore $e^{-F(t)} = \sin(2\gamma)$. Since the prefactor in (4.16) vanishes when $|t| = \gamma$, we conclude that α must be chosen in such a way that $\cos(\alpha t)$ is non-zero for $|t| < \gamma$, but vanishes as $|t| = \gamma$. This uniquely determines α to be $\alpha = \frac{\pi}{2\gamma}$. We obtain the final expression

$$e^{-F(t)} = \sin(\gamma - t)\sin(\gamma + t)\frac{\pi/2\gamma}{\cos(\pi t/2\gamma)}. \tag{4.18}$$

As a consistency check, one takes the limit $t \to \pm\gamma$ and finds $e^{-F(t)} = \sin(2\gamma)$, as it should be. Also, note that for $\gamma = \pi/4$, where the partition function is known and independent of t, one finds indeed that $e^{-F(t)} = 1$.

For further checks, let us set $t = 0$; a more standard normalization of the weights is then

$$a = b = 1 \qquad c = 2\cos\gamma \tag{4.19}$$

and the bulk free energy becomes

$$e^{-F} = \frac{\pi}{2}\frac{\sin\gamma}{\gamma}. \tag{4.20}$$

At $\gamma = \pi/6$, $\pi/4$, $\pi/3$, the values predicted by (4.20) coincide with the large-N limit of the expressions of [30]. Also, this fits perfectly with some numerical computations of the determinant we have performed.

We can compute the bulk energy (energy per unit site), which turns out to be

$$E = (\cot\gamma - 1/\gamma)\cot\gamma\log(2\cos\gamma). \tag{4.21}$$

Figure 5 shows the comparison with Monte Carlo simulations. The agreement is also very good.

Finally, let us mention that there seems to be no simple relation between the PBC and DWBC bulk free energies: from an analytic point of view, the DWBC free energy is an elementary function, whereas the PBC free energy is given by a non-trivial integral. Furthermore, the DWBC free energy is always greater then the PBC free energy, even at infinite temperature ($\Delta = \frac{1}{2}$), see figure 6.

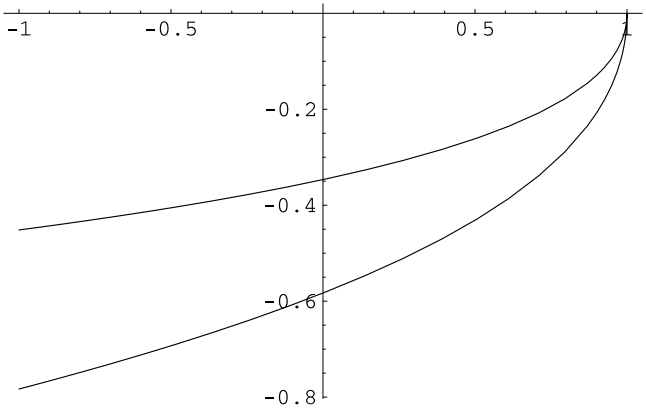

Figure 6. Bulk free energies for PBC and DWBC as a function of Δ.

4.3. Antiferroelectric phase: $\Delta < -1$

In this phase, the smoothness assumption of the sub-dominant corrections to the bulk free energy is *not* satisfied, as can be clearly seen numerically. The ratio $Z_{N+1}Z_{N-1}/Z_N^2$ does not converge in the large-N limit but instead has a pseudo-periodic behaviour reminiscent of the one-matrix model with several cuts [31], and slightly more sophisticated methods are needed to analyse the large-N limit. We leave this to a future publication.

4.4. Phase transition at $\Delta = 1$

If the Boltzmann weights depend on a parameter (e.g. temperature), it is known that with periodic boundary conditions, the system undergoes phase transitions as Δ crosses ± 1. Let us use the expressions of the bulk free energy found above to clarify what happens in the case of domain wall boundary conditions.

Here we shall consider the transition from ferroelectric (low-temperature) to disordered (high-temperature) regime, that is from $\Delta > 1$ to $\Delta < 1$. The parameter that plays the role of deviation from criticality $T - T_c$ can be defined as

$$T - T_c \equiv 1 - \Delta. \tag{4.22}$$

We assume that $b > a$ (the case $a > b$ can be treated similarly), and rescale the weights so that $b = 1$. With this convention, we simply have in the ferroelectric phase:

$$\mathrm{e}^{-F} = 1 \qquad \Delta > 1 \tag{4.23}$$

(cf equation (4.10)). Let us now consider $\Delta \to 1^-$. The weights are

$$a = \frac{\sin(\gamma - t)}{\sin(\gamma + t)} \qquad b = 1 \qquad c = \frac{\sin(2\gamma)}{\sin(\gamma + t)} \tag{4.24}$$

with $\gamma = \pi/2 + \epsilon$, $t = \pi/2 + \epsilon x$; x must be kept fixed as $\epsilon \to 0$. Note that $\Delta = \cos(2\epsilon)$, so that

$$T - T_c \propto \epsilon^2. \tag{4.25}$$

Expanding the expression (4.18) for the free energy, we obtain

$$\mathrm{e}^{-F} = 1 - \frac{2(x-1)^2}{3\pi}\epsilon^3 + \mathrm{O}(\epsilon^4). \tag{4.26}$$

Comparing (4.23) and (4.26), we find a *second-order* phase transition, with a singular part $(T - T_c)^{3/2}$ corresponding to a critical exponent $\alpha = -\frac{1}{2}$. This is to be contrasted with the first-order phase transition that occurs in the case of PBC. Let us, however, emphasize that the difference of orders of the phase transitions is not that significant, since the phase transition is somewhat special (in the case of PBC, the correlation length jumps from zero for $\Delta > 1$ to infinity for $\Delta < 1$).

5. Some equivalences

We shall now review some alternative interpretations of the partition function of the six-vertex model with domain wall boundary conditions; these equivalent formulations will shed some light on the property of dependence on boundary conditions that was found.

5.1. Alternating sign matrices

Six-vertex model arrow configurations with domain wall boundary conditions on an $N \times N$ lattice are in one-to-one correspondence with *alternating sign matrices* (ASM) of size N, that is square matrices with entries 0 or ± 1 such that each row and column has an alternating sequence of +1 and -1 (zeros excluded) starting and ending with a +1. Recalling that there are six weights which we shall call a_1, a_2, b_1, b_2, c_1, c_2 in the order shown in equation (2.2), the correspondence goes as follows: given a six-vertex configuration, assign a 0 to each vertex a or b and +1 (respectively -1) to each vertex c_1 (respectively c_2). One can show that this map is bijective, and therefore, the number of ASM is exactly equal to the partition function considered before with $a = b = c = 1$. For our purposes, let us define a refined counting of ASM (x-enumeration in the language of [30]) by assigning a weight x to each entry -1 of the ASM. The resulting quantity $A(N, x)$ is still related to the six-vertex model; indeed, one can easily show that

$$A(N, x) = x^{-N/2} Z_N(a = b = 1, c = \sqrt{x}). \tag{5.1}$$

If $0 \leqslant x \leqslant 4$, one can set $x = 4\cos^2\gamma$ and the weights are of the form (4.19). One can then prove (extending slightly the asymptotic expansion found in (4.2) that

$$\log A(N, x) = N^2 \log\left[\frac{\pi}{2}\frac{\sin\gamma}{\gamma}\right] - \frac{N}{2}\log x + \mathrm{O}(\log N) \qquad \forall x \in [0, 4]. \tag{5.2}$$

Though this equivalence does not directly provide any useful insight into the issue addressed in this paper, the result (5.2) itself might be of some mathematical interest.

5.2. Tilings of the Aztec diamond

A more illuminating equivalence is that of domino tilings (i.e. dimers on a square lattice in a dual description) and the six-vertex model at $\Delta = 0$—both models are well known to describe essentially one Dirac fermion. This is illustrated in figure 7. Since each vertex of type c_1 has two possible corresponding domino tiling configurations, one must assign it a Boltzmann weight of 2 in order to count each domino tiling exactly once; however, with most boundary conditions there are as many vertices of type c_1 and c_2, and therefore one can give them both a weight of $\sqrt{2}$ instead, which leads to the values $a = b = 1$, $c = \sqrt{2}$ of the parameters.

The more precise statement is that the number of domino tilings of the *Aztec diamond* (see [11]) is equal (up to a small known prefactor) to the partition function of the six-vertex model with domain wall boundary conditions at $a = b = 1$, $c = \sqrt{2}$ (see figure 8).

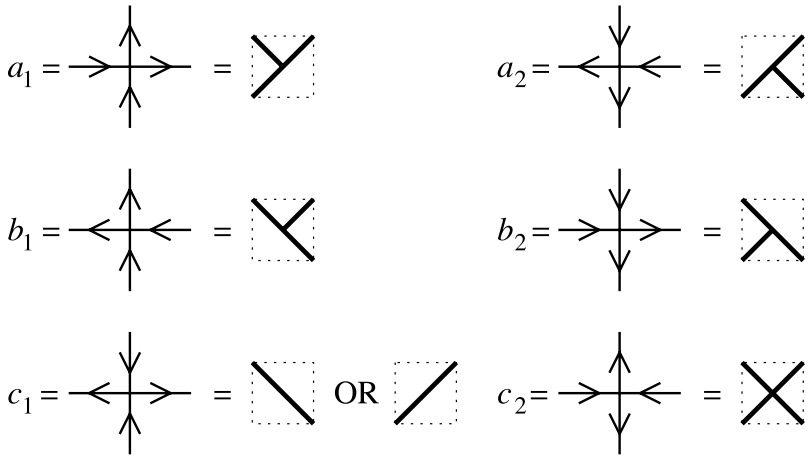

Figure 7. Correspondence between vertices of the six-vertex model and small patches of a domino tiling.

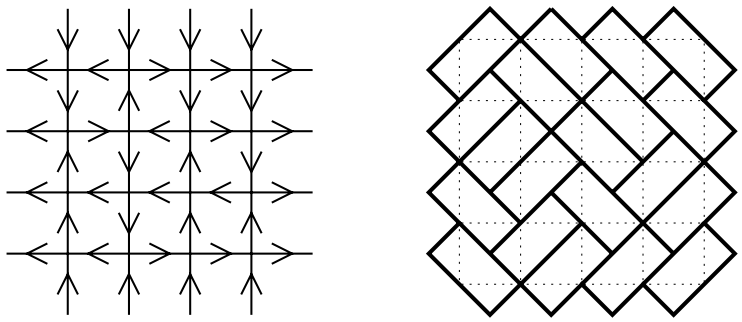

Figure 8. (*a*) A configuration of the six-vertex model with DWBC and (*b*) one possible corresponding tiling of the Aztec diamond.

Since this a local correspondence of configurations it extends to all correlation functions. Also, introducing some weights for the local tiling patterns amounts to changing the weights a, b, c, but always in such a way that Δ remains zero.

These tilings have been an object of interest for mathematicians, see in particular [12, 18]. The 'arctic circle theorem' [11] shows that as the size of the system grows large, the domino configurations become frozen outside the circle inscribed inside the diamond, and remain disordered but still heterogeneous [12] (i.e. non-translationally invariant) inside the circle. These statements have a straightforward equivalent in the six-vertex language: we expect the one-point functions of the six-vertex model at $\Delta = 0$ with DWBC to be non-constant (following a similar pattern as the tilings), and presumably a similar behaviour at $\Delta \neq 0$. This gives a qualitative understanding of the dependence of the bulk free energy on the boundary conditions.

5.3. Height model

The general eight-vertex is well known to be equivalent to a class of height models (SOS/RSOS model). In the case of the six-vertex model, there is a particularly simple equivalence which goes as follows: given a six-vertex configuration, integers are assigned to each face of the lattice in such a way that going from one face to a neighbouring face, the number is increased by one if the arrow in between goes right (and so, is decreased by one if it goes left). Conservation of the arrows ensures consistency of this procedure. The Boltzman weights of the model are simply the weights of the original six-vertex model expressed in terms of the new height variables.

This equivalence is particularly interesting because it gives us a simple intuitive explanation of the lack of thermodynamic limit due to boundary conditions; this was studied in detail and proven rigorously in the case of tilings ($\Delta = 0$), see [13]. Let us consider the domain wall boundary conditions and translate these into the language of our height model. They are fixed boundary conditions for the heights, of the form:

$$\begin{array}{ccccccc} 0 & & 1 & \cdots & N-1 & & N \\ 1 & & & & & & N-1 \\ \vdots & & & & & & \vdots \\ N-1 & & & & & & 1 \\ N & & N-1 & \cdots & 1 & & 0 \end{array}$$

where we have fixed arbitrarily the upper left height to be zero.

In the thermodynamic limit $N \to \infty$, let us define the rescaled coordinates on the square lattice to be $x = ka$, $y = \mathrm{i}a$, where $a \equiv 1/N$ is the lattice spacing. The heights $h_{i,j}$ are supposed to renormalize, according to standard lore, to a free massless bosonic field:

$$h_{i,j} \to \phi(x, y). \tag{5.3}$$

However, it is reasonable to assume that in order to have a proper thermodynamic limit, the boundary conditions must be well defined in terms of the limiting field ϕ. In the case of DWBC, one finds that the boundary conditions become $\phi(x, 0) = x/a$, etc, which do not have a limit as $a \to 0$; in particular, the variations of ϕ on the boundary diverge. More generally, we can conjecture that only the boundary conditions such that the variation of the function ϕ on the boundary can remain bounded will lead to the usual thermodynamic limit. This is essentially what is proven in [13] in the case $\Delta = 0$.

6. Conclusion

In this work, we have computed explicitly the large-N asymptotic behaviour of an $N \times N$ determinant which plays the role of partition function of the six-vertex model with domain wall boundary conditions. This gives rise to particularly simple expressions for the bulk free energy of this model (equations (4.10) and (4.18)). One important question is to physically interpret the discrepancy of the bulk free energy found when comparing domain wall and periodic boundary conditions of the six-vertex model, which is somewhat contrary to standard lore on the thermodynamic limit of statistical models. Some clues were given in the previous section, where various equivalences were discussed. In particular, it was shown how 'generic' fixed boundary conditions for the six-vertex model do not lead to a well defined thermodynamic limit. It would be useful to make these arguments more rigorous. Also, it would be most interesting to find a more quantitative description of the non-translational invariance created by the boundary conditions, and in particular to prove a 'generalized arctic circle theorem' for any value of the parameter Δ of the six-vertex model.

Acknowledgments

It is a pleasure to acknowledge stimulating discussions with E Lieb, F Y Wu, S Ruijsenaars (who informed us that he had similar results) and R Behrend (who participated in the early stages of this project). This work was supported by the National Science Foundation under grant no PHY-9605226 (VK).

References

[1] Lieb E 1967 *Phys. Rev. Lett.* **18** 692
[2] Lieb E 1967 *Phys. Rev. Lett.* **18** 1046
[3] Lieb E 1967 *Phys. Rev. Lett.* **19** 108
[4] Lieb E 1967 *Phys. Rev.* **162** 162
[5] Sutherland B 1967 *Phys. Rev. Lett.* **19** 103
[6] Baxter R J *Exactly Solved Models in Statistical Mechanics* (New York: Academic)
[7] Batchelor M T, Baxter R J, O'Rourke M J and Yung C M 1995 *J. Phys. A: Math. Gen.* **28** 2759
[8] Kasteleyn P W 1960 *Physica* **27** 1209
[9] Fisher M E 1961 *Phys. Rev.* **124** 1664
[10] Lu W T and Wu F Y 1999 *Phys. Lett.* A **259** 108
[11] Jockush W, Propp J and Shor P 1998 *Preprint* math. CO/9801068
[12] Cohn H, Elkies N and Propp J 1996 *Duke Math. J.* **85** 117
[13] Kenyon R, The planar dimer model with boundary: a survey *Preprint* (http://topo.math.u-psud.fr/∼kenyon/papers.html)
[14] Korepin V E 1982 *Commun. Math. Phys.* **86** 391
[15] Izergin A G 1987 *Sov. Phys.–Dokl.* **32** 878
[16] Izergin A G, Coker D A and Korepin V E 1992 *J. Phys. A: Math. Gen.* **25** 4315
[17] Sogo K 1993 *J. Phys. Soc. Japan* **62 6** 1887
[18] Elkies N, Kuperberg G, Larsen M and Propp J 1922 *J. Algebr. Comb.* **1** 111
Elkies N, Kuperberg G, Larsen M and Propp J 1922 *J. Algebr. Comb.* **1** 219
[19] Bressoud D M 1999 *Proofs and Confirmations: the Story of the Alternating Sign Matrix Conjecture* (Cambridge: Cambridge University Press)
[20] Bressoud D and Propp J 1999 *Not. AMS* 637
[21] Toda M 1967 *J. Phys. Soc. Japan* **22** 431
Toda M 1970 *Prog. Theor. Phys. Suppl.* **45** 174
[22] Hirota R 1987 *J. Phys. Soc. Japan* **56** 4285
[23] Flaschka H 1974 *Phys. Rev.* B **9**
Flaschka H 1974 *Prog. Theor. Phys.* **51** 703
[24] Ueno K and Takasaki K 1984 *Adv. Stud. Pure Math.* **4** 1
[25] Adler M and van Moerbeke P 1995 *Duke Math. J.* **80** 863
(Adler M and van Moerbeke P 1997 *Preprint* solv-int/9706010)
Adler M and van Moerbeke P 1999 *Preprint* math. CO/9912143
[26] Lipan O, Wiegmann P B, Zabrodin A 1997 *Preprint* solv-int/9704015
[27] Wiegmann P B, Zabrodin A 1999 *Preprint* hep-th/9909147
[28] Krichever I, Lipan O, Wiegmann P and Zabrodin A 1996 *Preprint* hep-th/9604080
[29] Gerasimov A, Marshakov A, Mironov A, Morozov A and Orlov A 1991 *Nucl. Phys.* B **357** 565
[30] Kuperberg G 1996 *Int. Math. Res. Not.* **3** 139
(Kuperberg G 1997 *Preprint* math. CO/9712207)
[31] Deift P, Kriecherbauer T, McLaughlin K T-R, Venakides S and Zhou X 1999 *Commun. Pure Appl. Math.* **52** 1491